# Dependence of Reaction Rates for Bidirectional PCET on Electron Donor – Electron Acceptor Distance in Phenol – Ru(2,2'-Bipyridine)<sub>3</sub><sup>2+</sup> Dyads

Jing Chen,† Martin Kuss-Petermann,† and Oliver S. Wenger\*

Department of Chemistry, University of Basel, St. Johanns-Ring 19, CH-4056 Basel, Switzerland oliver.wenger@unibas.ch

RECEIVED DATE (to be automatically inserted after your manuscript is accepted if required according to the journal that you are submitting your paper to)

† These two authors contributed equally.

# **ABSTRACT**

A homologous series of three donor-bridge-acceptor molecules in which a phenolic unit is attached covalently to a Ru(bpy)<sub>3</sub><sup>2+</sup> (bpy = 2,2'-bipyridine) complex via rigid rod-like p-xylene spacers was investigated. Photoexcitation at 532 nm in presence of large excess of methyl viologen leads to rapid (< 10 ns) formation of Ru(bpy)<sub>3</sub><sup>3+</sup>. When imidazole base is present in CH<sub>3</sub>CN solution, intramolecular electron transfer from the phenol to Ru(bpy)<sub>3</sub><sup>3+</sup> occurs, and this is coupled to proton transfer from the phenol to imidazole. All mechanistic possibilities for this proton-coupled electron transfer (PCET) process are considered, and based on a combination of kinetic and thermodynamic data one arrives at the conclusion that electron and proton release by the phenol occur in concert. By varying the number of p-xylene bridging units it then becomes possible to investigate the dependence of the reaction rates for concerted proton-electron transfer (CPET) on the phenol - Ru(bpy)<sub>3</sub><sup>3+</sup> distance. A distance decay constant of 0.87±0.09 Å<sup>-1</sup> is obtained. This is one of the largest β-values reported for electron transfer across oligo-p-phenylene based molecular bridges, but it is still relatively close to what was determined for "simple" (i. e., not proton-coupled) electron transfer across oligo-p-xylenes. Bidirectional concerted proton-electron transfer plays a key role in photosystem II. Understanding the distance dependence of such reactions is of interest for example in the context of separating protons and electrons across artificial membranes in order to build up charge gradients for light-to-chemical energy conversion.

# **KEYWORDS**

Proton transfer, electron transfer, photochemistry, transient absorption spectroscopy, luminescence spectroscopy

### INTRODUCTION

The dependence of electron transfer rates ( $k_{\rm ET}$ ) on the distance between an electron donor and an electron acceptor has been investigated for several decades, and many aspects of long-range electron transfer are now relatively well understood.<sup>1</sup> In the tunneling regime,  $k_{\rm ET}$  exhibits an exponential dependence on donor – acceptor distance, characterized by a distance decay constant ( $\beta$ ) which is strongly dependent on the intervening medium separating the donor from the acceptor.<sup>2</sup> For proton-coupled electron transfer (PCET) the dependence of reaction rates on the distance between individual reactants is much less well explored. Over the past few years the influence of the proton transfer distance on PCET rates has received significant attention, and in one experimental study it has been possible to determine a  $\beta$  value for the involved proton transfer event.<sup>3,4</sup> The dependence of PCET rates on electron donor – electron acceptor distance is beginning to be explored by several research groups, but until now there exist only a handful of studies on this specific subject.<sup>3,5,6</sup>

PCET can either occur via individual electron transfer and proton transfer steps (in whichever sequence) or in concerted fashion.<sup>7,8</sup> Concerted proton-electron transfer (CPET) is energy-conservative in the sense that high energy intermediates are avoided, making this mechanism particularly interesting.<sup>9,10</sup> Irrespective of the mechanism, PCET can be either unidirectional or bidirectional, meaning that electron and proton are transferred either from one reactant to another similar to hydrogenatom transfer (HAT) reactions, or the electron and the proton can be taken up by separate oxidants and bases. The dependence of rates for *unidirectional* CPET on electron donor – electron acceptor distance has recently been explored for the first time by Mayer and Gray.<sup>3</sup> We have recently reported the first experimental study of rates for *bidirectional* CPET as a function of electron donor – electron acceptor distance.<sup>5</sup> Here, we provide a significantly more detailed report of the influence of electron donor – electron acceptor distance on the rates for bidirectional CPET.

Our study is based on the three donor-bridge-acceptor molecules shown in Scheme 1. They are comprised of a phenolic unit which acts as a combined electron and proton donor, a variable number (1 – 3) of rigid rod-like *p*-xylene spacers, and a  $Ru(bpy)_3^{2+}$  (bpy = 2,2'-bipyridine) complex playing the role of a photosensitizer. Excess methyl viologen was used for the photogeneration of  $Ru(bpy)_3^{3+}$  in

order to trigger the PCET reaction in CH<sub>3</sub>CN. PCET can only occur in presence of base, e. g. with imidazole. From the sketch in Scheme 1 the bidirectional nature of the overall PCET process is evident. Variation of the number of *p*-xylene spacers permits phenol – ruthenium (center-to-center) distance variation between 12.2 and 20.8 Å. Related tyrosine – ruthenium and tyrosine – rhenium dyads have been investigated by several other research groups,<sup>11-25</sup> but to our knowledge the dependence of PCET rates on the tyrosine – metal distance has never been explored.

**Scheme 1.** Molecular structures of the three PhOH-xy<sub>n</sub>-Ru<sup>2+</sup> dyads investigated in this work. Photoexcitation in presence of methyl viologen and imidazole induces intramolecular electron transfer (ET) occurring in concert with intermolecular proton transfer (PT).

In this paper we will thoroughly consider all mechanistic possibilities for phototriggered PCET in the reaction systems from Scheme 1. We will show that concerted proton-electron transfer is indeed the most plausible reaction mechanism, and we will determine a distance decay constant for bidirectional CPET across p-xylene spacers and compare it to  $\beta$  values obtained in prior studies of "simple" (i. e., not proton-coupled) electron transfer across comparable molecular bridges. We will close with a few general thoughts and conclusions regarding the dependence of CPET rates on electron donor – electron acceptor distances.

### **RESULTS**

Cyclic voltammograms of the three donor-bridge-acceptor molecules from Scheme 1 and the Ru(bpy)<sub>3</sub><sup>2+</sup> reference complex measured in dry CH<sub>3</sub>CN are shown in Figure 1. The reversible waves at 0.0 V vs Fc<sup>+</sup>/Fc are due to ferrocene which was added in small amounts for internal voltage calibration. All voltammograms were recorded in presence of 0.1 M TBAPF<sub>6</sub> at scan rates of 100 mV/s. In the potential range considered here, most of the detectable waves are due to the Ru(bpy)<sub>3</sub><sup>2+</sup> complex.

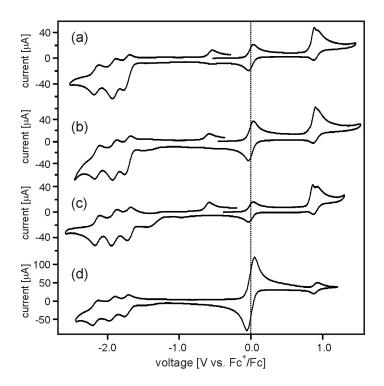


**Figure 1.** Cyclic voltammograms of (a) PhOH-xy<sub>1</sub>-Ru<sup>2+</sup>, (b) PhOH-xy<sub>2</sub>-Ru<sup>2+</sup>, (c) PhOH-xy<sub>3</sub>-Ru<sup>2+</sup>, and (d) Ru(bpy)<sub>3</sub><sup>2+</sup> in CH<sub>3</sub>CN with 0.1 M TBAPF<sub>6</sub>. The voltage sweep rate was 0.1 V/s; the reversible wave at 0.0 V is due to ferrocene which was added in small quantities for voltage calibration.

Specifically, oxidation of Ru(II) to Ru(III) occurs at about 0.9 V vs. Fc<sup>+</sup>/Fc (Figure 1d) whereas oneelectron reduction of the three bpy ligands takes places at potentials between -1.7 and -2.2 V vs. Fc<sup>+</sup>/Fc, as commonly observed.<sup>26</sup> Careful inspection of the dyad voltammograms (Figure 1a – 1c) reveals an additional oxidation wave near 0.9 V vs. Fc<sup>+</sup>/Fc next to the ruthenium oxidation wave; this is particularly evident in Figure 1c but the additional wave is also present in Figures 1a/1b. This additional wave is attributed to phenol oxidation which is irreversible,<sup>27,28</sup> presumably due to proton loss.<sup>29</sup> The three dyads further exhibit an additional wave near -0.6 V vs. Fc<sup>+</sup>/Fc which only appears after an initial oxidative sweep to potentials above 0.9 V vs. Fc<sup>+</sup>/Fc. We attribute this wave to oxidation of phenolate (PhO<sup>-</sup>) to phenoxyl radical (PhO•).<sup>30</sup> Table 1 lists the pertinent reduction potentials extracted from Figure 1 along with two relevant potentials of the 2,4,6-tri-*tert*.-butyl-phenol (2,4,6-'Bu<sub>3</sub>PhOH) reference molecule taken from the literature.<sup>28</sup> In Table 1, only the first reduction potentials for the Ru(bpy)<sub>3</sub><sup>2+</sup> complexes are listed, and these potentials are labelled with  $E^0(\text{Ru}^{2+}/\text{Ru}^+)$  for simplicity even though this reduction is ligand-centered.

**Table 1.** Reduction potentials (in V vs. Fc<sup>+</sup>/Fc in CH<sub>3</sub>CN) for one-electron reduction of the individual molecular components.

molecule	$E^0(Ru^{3+}/Ru^{2+})$	$E^0(Ru^{2+}/Ru^+)$	E <sup>0</sup> (PhOH <sup>+</sup> /PhOH)	$E^{\theta}(\text{PhO}\bullet/\text{PhO}^{-})$
PhOH-xy <sub>1</sub> -Ru <sup>2+</sup>	0.90	-1.73	0.88	-0.54
_				
PhOH-xy <sub>2</sub> -Ru <sup>2+</sup>	0.90	-1.72	0.90	-0.58
PhOH-xy <sub>3</sub> -Ru <sup>2+</sup>	0.88	-1.72	0.86	-0.58
$Ru(bpy)_3^{2+}$	0.86	-1.72		
2,4,6- <sup>t</sup> Bu <sub>3</sub> PhOH			1.18	-0.70

Data extracted from cyclic voltammograms shown in Figure 1, except those of 2,4,6- $^{4}$ Bu<sub>3</sub>PhOH which were taken from the literature. The first reduction of the Ru(bpy)<sub>3</sub><sup>2+</sup> complex is ligand-based and is only for simplicity labelled with  $E^{0}$ (Ru<sup>2+</sup>/Ru<sup>+</sup>).

The solid black lines in Figure 2 are the optical absorption spectra of the three dyads from Scheme 1 in CH<sub>3</sub>CN. They are dominated by the  ${}^{1}$ MLCT absorption band of the Ru(bpy)<sub>3</sub><sup>2+</sup> moiety at 450 nm, and a bpy-centered  $\pi$ - $\pi$ \* transition around 290 nm. The dyad spectra differ rather little from the spectrum of free Ru(bpy)<sub>3</sub><sup>2+</sup>. Addition of excess TBAOH (tetra-*n*-butylammonium hydroxide) leads to deprotonation of the phenolic units, and the absorption spectra of the resulting phenolate forms of the three dyads are shown as red traces in Figure 2. The phenolate forms exhibit additional absorption bands near 350 nm

and at wavelengths longer than 500 nm. The Ru(bpy)<sub>3</sub><sup>2+</sup>-localized MLCT state appears to be no longer the lowest energetic electronically excited state in the deprotonated dyads.

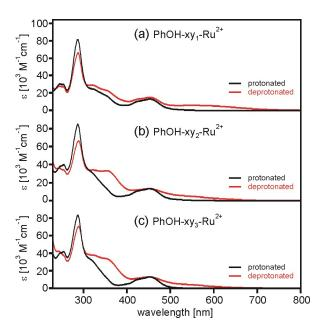


**Figure 2.** UV-Vis absorption spectra of the three dyads (black traces) and their deprotonated phenolate forms (red traces) in CH<sub>3</sub>CN. Deprotonation occurred by adding excess TBAOH.

The protonated forms of the three dyads exhibit luminescence from the lowest lying <sup>3</sup>MLCT state upon excitation at 450 nm in CH<sub>3</sub>CN (Figure S1). In the deprotonated forms the emission is nearly completely quenched, suggesting that the <sup>3</sup>MLCT state is indeed no longer the lowest-energetic electronically excited state, as suspected based on the absorption spectra. The <sup>3</sup>MLCT luminescence lifetime of the protonated forms in aerated CH<sub>3</sub>CN is approximately 200 ns (Figure S2), similar to what is measured for the Ru(bpy)<sub>3</sub><sup>2+</sup> reference complex under identical conditions. The very weak remaining luminescence of the deprotonated dyads decays with an instrumentally limited lifetime of ~10 ns (Figure S2).

Imidazole does not react with photoexcited  $Ru(bpy)_3^{2+}$  (Figure S3), but methyl viologen (MV<sup>2+</sup>) quenches the <sup>3</sup>MLCT excited state of the protonated dyads with similar efficiency as it quenches the <sup>3</sup>MLCT state of free  $Ru(bpy)_3^{2+}$ . The black and blue lines in Figure 3 are transient difference spectra

measured after excitation of 2·10<sup>-5</sup> M solutions of the three dyads from Scheme 1 in CH<sub>3</sub>CN in presence of 80 mM methyl viologen (MV<sup>2+</sup>) hexafluorophosphate and in presence of imidazole (im) base. The imidazole concentration was 20 mM in the case of PhOH-xy<sub>1</sub>-Ru<sup>2+</sup> and 200 mM for the two longer dyads. Laser pulses of ~10 ns duration at 532 nm were used for excitation, detection of the spectra occurred by time-integrating the signal on an iCCD camera over a time period of 200 ns.

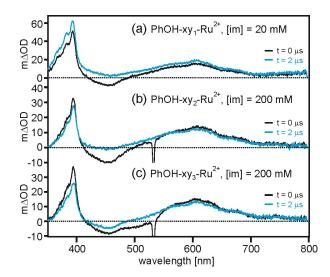
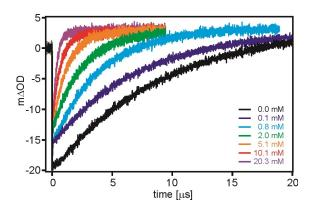


Figure 3. Transient difference spectra for  $2 \cdot 10^{-5}$  M solutions of the dyads in presence of 80 mM methyl viologen and 20 - 200 mM imidazole after excitation at 532 nm with pulses of ~10 ns duration. The black traces were recorded by time-averaging over the first 200 ns immediately after excitation. The blue traces were measured with a time delay of 2  $\mu$ s and time-averaging over the subsequent 200 ns.

The black lines are spectra which were measured in the first 200 ns immediately after the laser pulses, while the blue lines are spectra which were recorded after a time delay of 2 μs. The most prominent features of all 6 transient absorption spectra are a relatively narrow band at 395 nm and a broader band centered around 605 nm, which are characteristic features of one-electron reduced methyl viologen (MV\*+).<sup>31</sup> The spectra recorded without time delay (black lines) additionally exhibit a negative signal near 450 nm which is characteristic for the oxidized ruthenium complex (Ru(bpy)<sub>3</sub><sup>3+</sup>); this spectral

feature is often referred to as the MLCT bleach.  $^{15,23,32-34}$  Thus, photoexcitation of the dyads in presence of imidazole and methyl viologen induces electron transfer from their  $^3$ MLCT-excited Ru(bpy) $_3^{2+}$  moieties to methyl viologen. In the spectra of PhOH-xy<sub>1</sub>-Ru<sup>2+</sup> and PhOH-xy<sub>2</sub>-Ru<sup>2+</sup> recorded with 2 µs time delay (blue lines) the bleach at 450 nm has disappeared but the signals at 395 and 605 nm are still present, indicating that Ru(bpy) $_3^{3+}$  disappears more rapidly than MV\*+. $_3^{5-}$ 



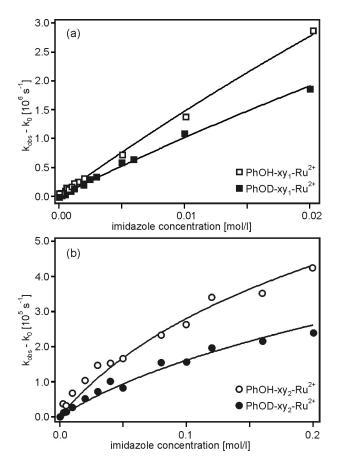
**Figure 4.** Recovery of the <sup>1</sup>MLCT bleach after 532-nm excitation of a 2·10<sup>-5</sup> M solution of PhOH-xy<sub>1</sub>-Ru<sup>2+</sup> in CH<sub>3</sub>CN with 80 mM methyl viologen and various concentrations of imidazole.

Figure 4 shows the temporal evolution of the MLCT bleach at 450 nm after excitation of the PhOH-xy<sub>1</sub>-Ru<sup>2+</sup> dyad in aerated CH<sub>3</sub>CN in presence of 80 mM MV<sup>2+</sup> and increasing concentrations of imidazole. The excitation wavelength was 532 nm, the pulse width was ~10 ns. Analogous data sets for the two longer dyads are shown in the Supporting Information (Figure S4). The general observation for all three dyads is that the MLCT bleach recovers more rapidly with increasing imidazole concentration, and in all cases single exponential decay curves are measured. However, the longer the *p*-xylene bridge becomes, the more imidazole is required to accelerate the MLCT bleach recovery. For instance, in the PhOH-xy<sub>1</sub>-Ru<sup>2+</sup> dyad the bleach recovery time (based on a single exponential fit) is 1.2 μs at an imidazole concentration of 5 mM (Figure 4), but for the PhOH-xy<sub>2</sub>-Ru<sup>2+</sup> dyad an imidazole concentration of 200 mM can only accelerate the MLCT bleach recovery to 1.7 μs (Figure S4c). In the

PhOH-xy<sub>3</sub>-Ru<sup>2+</sup> dyad addition of imidazole has an even weaker effect (Figure S4e). In the case of PhOH-xy<sub>3</sub>-Ru<sup>2+</sup> the acceleration of the MLCT bleach recovery induced by imidazole is within experimental accuracy the same as that observed for the Ru(bpy)<sub>3</sub><sup>2+</sup> reference complex (Figure S4g); an increase in the imidazole concentration from 0 to 200 mM can only induce a change in bleach recovery time from ~40 μs to ~14 μs for PhOH-xy<sub>3</sub>-Ru<sup>2+</sup> and Ru(bpy)<sub>3</sub><sup>2+</sup>. A Stern-Volmer experiment monitoring the MLCT bleach recovery time as a function of imidazole concentration (Figure S6) shows that Ru(bpy)<sub>3</sub><sup>3+</sup> (in contrast to photoexcited Ru(bpy)<sub>3</sub><sup>2+</sup> (Figure S3)) reacts with imidazole with a rate constant of 5.6·10<sup>5</sup> M<sup>-1</sup> s<sup>-1</sup>. While this rate constant can fully account for the acceleration of MLCT bleach recoveries detected for PhOH-xy<sub>3</sub>-Ru<sup>2+</sup> in presence of imidazole, it is clear that the bleach recoveries detected for PhOH-xy<sub>1</sub>-Ru<sup>2+</sup> and PhOH-xy<sub>2</sub>-Ru<sup>2+</sup> are too fast to be explained by direct interaction of their Ru(bpy)<sub>3</sub><sup>3+</sup> moieties with imidazole.

When replacing the phenolic protons and the easily exchangeable imidazole N-H protons by deuterons, the MLCT bleach recovery kinetics characterizing the disappearance of Ru(bpy)<sub>3</sub><sup>3+</sup> in the PhOH-xy<sub>1</sub>-Ru<sup>2+</sup> and PhOH-xy<sub>2</sub>-Ru<sup>2+</sup> dyads are somewhat changed (Figure S4b/d). At a given imidazole concentration, the bleach recoveries are slower than before deuteration. In other words, there is an H/D kinetic isotope effect (KIE; 1.5±0.5 for PhOH-xy<sub>1</sub>-Ru<sup>2+</sup>, 2.1±0.6 for PhOH-xy<sub>1</sub>-Ru<sup>2+</sup>, see below), indicating that reduction of Ru(bpy)<sub>3</sub><sup>3+</sup> is coupled to a proton transfer step.

In Figure 5a the acceleration of the MLCT bleach recoveries is shown as a function of the imidazole concentration for the shortest dyad (PhOH- $xy_1$ - $Ru^{2+}$ , open squares) and its deuterated analog (PhOD- $xy_1$ - $Ru^{2+}$ , filled squares). Specifically, we plot  $k_{obs} - k_0$ , i. e., the difference between the bleach recovery time in presence of a given concentration of imidazole ( $k_{obs}$ ) and the inherent bleach recovery measured in pure CH<sub>3</sub>CN containing no imidazole ( $k_0$ ). The H/D kinetic isotope effect mentioned above is readily visible from the data in Figure 5a. In Figure 5b analogous sets of data for PhOH- $xy_2$ - $Ru^{2+}$  (open circles) and PhOD- $xy_2$ - $Ru^{2+}$  (filled circles) are shown.



**Figure 5.** Dependence of <sup>1</sup>MLCT bleach recovery rate of PhOH/D-xy<sub>1</sub>-Ru<sup>2+</sup> and PhOH/D-xy<sub>2</sub>-Ru<sup>2+</sup> in CH<sub>3</sub>CN with 80 mM methyl viologen on the imidazole concentration. k<sub>obs</sub> is the experimentally observable rate in presence of imidazole (extracted from the data in Figures 4 / S4), k<sub>0</sub> is the experimentally observable rate for a given dyad in absence of imidazole. The solid lines are fits with eq. 4 to the experimental data yielding the CPET rate constants in Table 3.

# **DISCUSSION**

Photochemistry in presence of  $MV^{2+}$  and imidazole. Up to concentrations of 0.4 M, imidazole has no detectable influence on the  ${}^{3}$ MLCT emission of Ru(bpy) ${}_{3}^{2+}$  (Figure S3). However, the emissive  ${}^{3}$ MLCT excited state of Ru(bpy) ${}_{3}^{2+}$  in CH ${}_{3}$ CN is quenched oxidatively by methyl viologen with a rate constant of  $2.4 \cdot 10^{9}$  M ${}^{-1}$  s ${}^{-1}$ . ${}^{36}$  Thus, when 80 mM of MV ${}^{2+}$  is present, Ru(bpy) ${}_{3}^{3+}$  and MV ${}^{++}$  can be formed within less than 5 ns. Indeed the transient absorption spectra in Figure 3 recorded without time delay (black trace) provide evidence for these two species in the form of a bleach at 450 nm (due to Ru(bpy) ${}_{3}^{3+}$ ) ${}^{37}$  and

absorption bands at 395 and 605 nm (due to MV\*+).<sup>31</sup> 2 μs later the bleach at 450 nm has essentially disappeared (at least in the PhOH-xy<sub>1</sub>-Ru<sup>2+</sup> and PhOH-xy<sub>2</sub>-Ru<sup>2+</sup> dyads), but the signals at 395 and 605 nm are still present (blue traces in Figure 3). As noted above, this indicates that Ru(bpy)<sub>3</sub><sup>3+</sup> disappears more rapidly than MV\*+.

Ru(bpy)<sub>3</sub><sup>3+</sup> reacts with imidazole in an undesired side reaction, presumably leading to oxidation of imidazole and formation of Ru(bpy)<sub>3</sub><sup>2+</sup> (Figure S6).<sup>38</sup> However, given our experimentally determined rate constant of 5.6·10<sup>5</sup> M<sup>-1</sup> s<sup>-1</sup> (Supporting Information), the bimolecular reaction between Ru(bpy)<sub>3</sub><sup>3+</sup> and imidazole cannot account for a bleach recovery time of ~350 ns in PhOH-xy<sub>1</sub>-Ru<sup>2+</sup> in presence of 20 mM imidazole (Figure 4) or a bleach recovery time of ~1700 ns in PhOH-xy<sub>2</sub>-Ru<sup>2+</sup> in presence of 200 mM imidazole (Figure S4c). Consequently, yet another reaction must be responsible for the rapid disappearance of Ru(bpy)<sub>3</sub><sup>3+</sup> in PhOH-xy<sub>1</sub>-Ru<sup>2+</sup> and PhOH-xy<sub>2</sub>-Ru<sup>2+</sup> in presence of imidazole. Intramolecular electron transfer from phenol to Ru(bpy)<sub>3</sub><sup>3+</sup> (coupled to transfer of the phenolic proton to imidazole) is the only plausible option to account for the rapid bleach recovery kinetics. Several prior studies of tyrosine - ruthenium dyads in aqueous solutions using methyl viologen for the photogeneration of  $Ru(bpy)_3^{3+}$  have reached the same conclusion; in presence of base,  $Ru(bpy)_3^{3+}$  can oxidize tyrosine (and most other phenols) by intramolecular long-range electron transfer. 11-20,24,39 Similar observations have been made for tyrosine - rhenium and phenol - rhenium systems, for which PCET originates from an electronically excited state. 6,21,22,40 The neutral phenoxyl radicals which are formed as a result of this photoreaction usually remain undetected because they absorb around 400 nm with extinction coefficients on the order of 5000 M<sup>-1</sup> cm<sup>-1</sup>, <sup>41,42</sup> i. e., in a spectral range where MV\*+ has an extinction of approximately 17500 M<sup>-1</sup> cm<sup>-1</sup>.<sup>31</sup> From the spectra in Figure 3 it is equally clear that phenolate photoproducts are not formed; the phenolate forms would lead to new absorption bands around 550 nm with extinction coefficients on the order of 5000 M<sup>-1</sup> cm<sup>-1</sup> (red traces in Figure 2), which is of comparable magnitude as the  $MV^{\bullet+}$  extinction at 605 nm (~6000  $M^{-1}$  cm<sup>-1</sup>).<sup>31</sup>

Thus, the sequence of reactions shown in Scheme 2 is likely to occur after photoexcitation of the  $PhOH-xy_n-Ru^{2+}$  dyads in presence of  $MV^{2+}$  and imidazole. Following the initial laser flash, photoexcited

Ru(bpy)<sub>3</sub><sup>2+</sup> is quenched oxidatively by methyl viologen. The resulting Ru(bpy)<sub>3</sub><sup>3+</sup> species then abstracts an electron from phenol, and the phenolic proton is released to imidazole in an overall PCET reaction. The reaction products are phenoxyl radical (PhO•), Ru(bpy)<sub>3</sub><sup>2+</sup>, and protonated imidazole (imH<sup>+</sup>). We have not been able to determine the oxidation potential of imidazole nor have we found a value for it in the literature, but we suspect that in an undesired side reaction Ru(bpy)<sub>3</sub><sup>3+</sup> can oxidize imidazole. For the dyads with n = 1 and n = 2 the PCET step is more rapid than the undesired side reaction because the electron transfer distance is short enough, but in the dyad with n = 3 this is not the case anymore. For this reason the subsequent discussion will focus largely on the PhOH-xy<sub>1</sub>-Ru<sup>2+</sup> and PhOH-xy<sub>2</sub>-Ru<sup>2+</sup> dyads. The flash/quench procedure shown in Scheme 2 has been previously applied many times for studies of electron transfer in proteins, <sup>32,43,44</sup> donor-bridge-acceptor molecules, <sup>33,34,45</sup> and for PCET investigations. <sup>11-20,23</sup>

**Scheme 2.** Sequence of reactions occurring after photoexcitation of the PhOH- $xy_n$ -Ru<sup>2+</sup> dyads in CH<sub>3</sub>CN in presence of methyl viologen (MV<sup>2+</sup>) and imidazole. The experimentally observable photoproducts (Figure 3) are marked with a grey shaded background.

"flash" "quench" PCET

$$MV^{2+}$$
  $MV^{+}$  im  $imH^{+}$ 

PhOH- $xy_n$ - $Ru^{2+}$  PhOH- $xy_n$ - $Ru^{2+}$  PhOH- $xy_n$ - $Ru^{2+}$  im  $im^{+}$   $im$ 

Aside from the reaction sequence in Scheme 2 yet another scenario, illustrated by Scheme 3, is in principle conceivable. In a proton transfer pre-equilibrium PhO<sup>-</sup>-xy<sub>n</sub>-Ru<sup>2+</sup> and imH<sup>+</sup> could potentially be formed out of PhOH-xy<sub>n</sub>-Ru<sup>2+</sup> and imidazole. A flash-quench sequence could then lead to PhO<sup>-</sup>-xy<sub>n</sub>-Ru<sup>3+</sup> which could react onwards to the same photoproduct as above (PhO•-xy<sub>n</sub>-Ru<sup>2+</sup>). Alternatively, PhO<sup>-</sup>-xy<sub>n</sub>-\*Ru<sup>2+</sup> could react to PhO•-xy<sub>n</sub>-Ru<sup>+</sup>, followed by reduction of MV<sup>2+</sup> by Ru(bpy)<sub>3</sub>+, leading to

the same photoproducts. There are several arguments that speak strongly against the sequences of reactions shown in Scheme 3, and these arguments will be discussed in detail below.

**Scheme 3.** Pre-equilibrium between the phenol and phenolate forms of the PhOH-xy<sub>n</sub>-Ru<sup>2+</sup> dyads in CH<sub>3</sub>CN in presence of imidazole and subsequent possible photoreactions with the phenolate forms. The experimentally observable photoproducts are marked with a grey shaded background.

PhOH-
$$xy_n$$
- $Ru^{2+}$ 

PhO $-xy_n$ - $Ru^{2+}$ 

im

im

im

side

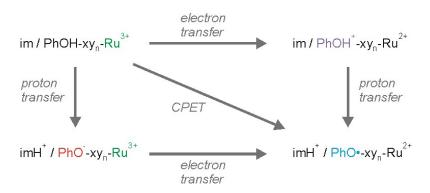
reaction

PhO $-xy_n$ - $Ru^{2+}$ 

*PCET mechanisms*. Assuming that the reaction sequence shown in Scheme 2 is correct (we will provide strong evidence for this below when we discuss all other possibilities on the basis of an energy level scheme), the starting point for the overall PCET reaction is the mixture comprised of imidazole and PhOH-xy<sub>n</sub>-Ru<sup>3+</sup> (top left corner of Scheme 4). PCET can then occur via three different mechanistic pathways.<sup>7</sup> In principle, there can first be a rate-determining electron transfer step (top right corner of Scheme 4) which is followed by proton transfer, but the opposite reaction sequence (passing along the bottom left corner of Scheme 4) is also conceivable. The third option is concerted proton-electron transfer across the diagonal of Scheme 4.

**Scheme 4.** The three possible mechanistic pathways for proton-coupled electron transfer (PCET) in the reaction system comprised of ruthenium-oxidized dyads and imidazole. The flash-quench generated PhOH-xy<sub>n</sub>-Ru<sup>3+</sup> species and neutral imidazole on the top left corner are the starting point for PCET, the PhO•-xy<sub>n</sub>-Ru<sup>2+</sup> dyads and protonated imidazole (imH<sup>+</sup>) at the bottom right are the experimentally

observable photoproducts. Reaction along the diagonal corresponds to concerted proton-electron transfer. Reactions along the corners are stepwise processes.



This last option is particularly interesting because it avoids the high-energy intermediates resulting from individual electron and proton transfer steps. In the following we will discuss which one of the three mechanistic options is the most probable for our PhOH-xy<sub>n</sub>-Ru<sup>2+</sup> dyads.

**Table 2.** Acidity constants of all relevant molecular components in various solvents.

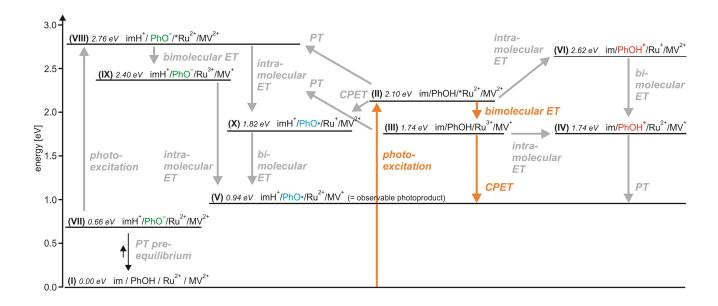
molecule	pK <sub>a</sub> in CH <sub>3</sub> CN	pKa in DMSO	pK <sub>a</sub> in H <sub>2</sub> O
2,4,6- <sup>t</sup> Bu <sub>3</sub> PhOH	29.8 <sup>a</sup>	17.8 <sup>b</sup>	13 <sup>b</sup>
2,4,6- <sup>t</sup> Bu <sub>3</sub> PhOH <sup>+</sup>	-3 <sup>b</sup>	-10 <sup>b</sup>	-5 <sup>b</sup>
imidazole (im)	30.5 <sup>a</sup>	18.6 <sup>b</sup>	13°
imidazolium (imH <sup>+</sup> )	18.6 <sup>a</sup>	6.4 <sup>d</sup>	7°

<sup>&</sup>lt;sup>a</sup> Calculated from the values in DMSO using the relationship pK<sub>a</sub>(CH<sub>3</sub>CN) = 12.31 + 0.98⋅pK<sub>a</sub>(DMSO).<sup>47</sup>; <sup>b</sup> From ref. <sup>28</sup>; <sup>c</sup> From ref. <sup>48</sup>; <sup>d</sup> From ref. <sup>49</sup>. Note that the imH<sup>+</sup> (and not the im) species is relevant for the CPET reaction considered in this work.

The mechanistic discussion can only be made properly when the thermodynamics of the individual reaction steps are known.<sup>7</sup> Based on the reduction potentials in Table 1 and the acidity constants in Table 2 it is possible to estimate the energies of all potentially relevant reaction products that can emerge from the reaction triple comprised of PhOH- $xy_n$ - $Ru^{2+}$ , imidazole, and methyl viologen ( $MV^{2+}$ )

in CH<sub>3</sub>CN. How exactly this is done is explained in detail in the Supporting Information, Scheme 5 merely summarizes the result. In the following we report energies with two digits but we note that our energy estimates are only accurate to  $\pm 0.1$  eV for electron transfer (ET) steps and to  $\pm 0.3$  eV for proton transfer (PT) steps.

**Scheme 5.** Energy-level diagram for the various possible photoproducts resulting from the reaction triple comprised of PhOH- $xy_n$ -Ru<sup>2+</sup>, methyl viologen (MV<sup>2+</sup>), and imidazole (im). The energies were estimated on the basis of redox potentials and acidity constants as described in the Supporting Information. The orange arrows mark the principal photochemical reaction pathway. ET = electron transfer, PT = proton transfer, CPET = concerted proton-electron transfer.



Following excitation of the Ru(bpy)<sub>3</sub><sup>2+</sup> moieties in the dyads, one reaches the <sup>3</sup>MLCT state at 2.10 eV above the ground state (state II in Scheme 5, orange upward arrow). <sup>36</sup> Bimolecular electron transfer with MV<sup>2+</sup> then leads to state III (orange downward arrow) at 1.74 eV, comprised of ordinary imidazole, PhOH-xy<sub>n</sub>-Ru<sup>3+</sup>, and MV<sup>++</sup>. From state III, proton transfer (PT) from PhOH-xy<sub>n</sub>-Ru<sup>3+</sup> to imidazole is endergonic by 0.66 eV (grey upward arrow to state IX). This energy estimate is based on the pK<sub>a</sub> values of 2,4,6-'Bu<sub>3</sub>PhOH (29.8) and imH<sup>+</sup> (18.6) in CH<sub>3</sub>CN (Table 2) and equation 1:<sup>7</sup>

$$\Delta G_{PT}^{0} = 0.059 \text{ eV} \cdot [pK_a(2,4,6-Bu_3PhOH) - pK_a(imH^+)]$$
 (eq. 1)

If one considers states III and IX to be in chemical equilibrium, the molar ratio between PhO<sup>-</sup>-xy<sub>n</sub>-Ru<sup>3+</sup> (in state IX) and PhOH-xy<sub>n</sub>-Ru<sup>3+</sup> (in state III) is  $6.9 \cdot 10^{-12}$ :1 (see Supporting Information for details). Even under the assumption that the rate constant for the exergonic proton transfer from imH<sup>+</sup> to PhO<sup>-</sup>-xy<sub>n</sub>-Ru<sup>3+</sup> is  $6 \cdot 10^{12}$  s<sup>-1</sup> (i. e., corresponding to the frequency factor of absolute rate theory),<sup>50</sup> the rate constant for the endergonic proton transfer from PhOH-xy<sub>n</sub>-Ru<sup>3+</sup> to imidazole is limited to  $6 \cdot 10^{12}$  s<sup>-1</sup> ×  $6.9 \cdot 10^{-12} = \sim 40$  s<sup>-1</sup>. Thus, the expected maximal rate constant for the proton transfer step from state III to state IX is  $\sim 40$  s<sup>-1</sup>, which is far too slow to account for the experimentally observable reaction kinetics. The same line of arguments holds for proton transfer from PhOH-xy<sub>n</sub>-\*Ru<sup>2+</sup> to imidazole, i. e., the reaction of state II to state VIII (grey upward arrow). Moreover, in view of the exergonic bimolecular ET with 80 mM MV<sup>2+</sup> (conversion of state II to state III with k =  $2.4 \cdot 10^9$  M<sup>-1</sup> s<sup>-1</sup>)<sup>36</sup> the PT step from state II to state VIII is particularly unlikely.

The considerations made above are also relevant regarding the proton transfer pre-equilibrium discussed in Scheme 3. In Scheme 5 this pre-equilibrium is included on the left bottom with state VII at 0.66 eV above the ground state. In principle, photoexcitation of the small subset of dyads which are in their phenolate forms could promote them from state VII to state VIII at 2.76 eV (grey upward arrow) from which a sequence of intra- and bimolecular reactions could subsequently lead to the observable photoproducts (state V at 0.94 eV). Based on the considerations from above the formation of the species in state VII (from state I) is not rapid enough to account for the observable reaction kinetics. What is more, the <sup>3</sup>MLCT state does not appear to be the lowest electronically excited state in the deprotonated dyads (see above), and consequently photoexcitation of PhO<sup>-</sup>-xy<sub>n</sub>-Ru<sup>2+</sup> at 532 nm is likely to lead to nonradiative relaxation without inducing any photochemistry at all.

The key conclusion until here is that a sequence of proton transfer followed by electron transfer, either via a PT pre-equilibrium (state VII in Scheme 5) or via rapid PT after initial <sup>3</sup>MLCT excitation (reaction from state II to state VIII or from state III to state IX) is very unlikely; the experimentally observable reaction kinetics as a function of imidazole concentration cannot be reconciled with either one of the two PT-ET scenarios (see also Supporting Information and attempted fits with PT-ET models). Neither one of the reaction sequences shown in Scheme 3 can be a viable reaction pathway.

The logical next question then is whether an ET-PT reaction sequence is possible. According to Scheme 5 two different ET-PT reaction sequences are conceivable. The first one would involve intramolecular electron transfer from phenol to photoexcited Ru(bpy)<sub>3</sub><sup>2+</sup> as an initial reaction step (state II to state VI in Scheme 5). However, this reaction is endergonic by 0.5 eV, hence in presence of 80 mM MV<sup>2+</sup> and the abovementioned rate constant for Ru(bpy)<sub>3</sub><sup>2+</sup> <sup>3</sup>MLCT quenching by MV<sup>2+</sup> (2.4·10<sup>9</sup> M<sup>-1</sup> s<sup>-1</sup> 1)36 intermolecular electron transfer from photoexcited Ru(bpy)32+ to MV2+ must be the dominant reaction pathway (orange downward arrow from state II to state III). Once the PhOH-xy<sub>n</sub>-Ru<sup>3+</sup> photoproducts are formed, there is essentially no driving force for intramolecular electron transfer from phenol to Ru(bpy)<sub>3</sub><sup>3+</sup> (horizontal grey arrow from state III to state IV) because the electrochemical potentials for oxidation of phenol and Ru(bpy)<sub>3</sub><sup>2+</sup> are nearly identical (Table 1). This equiergic electron transfer step is in competition with the CPET process marked by the orange downward arrow between state III and state V which is exergonic by 0.80 eV. Thus, the concerted release of an electron and a proton from the phenol is a far more plausible reaction pathway than an ET-PT reaction sequence. Furthermore, the experimentally observable H/D kinetic isotope effect (Figure 5) indicates that the rate determining step involves proton motion, and this is another argument against an ET-PT sequence with a rate determining electron transfer process.

In principle, direct photoinduced CPET from state II to state X, involving MLCT-excited Ru(bpy)<sub>3</sub><sup>2+</sup> (as the case in one of our prior studies)<sup>5</sup> represents yet another mechanistic option. However, at 80 mM methyl viologen concentration this CPET step is kinetically not competitive with oxidative quenching by  $MV^{2+}$  (Figure S6).

We conclude that after the flash/quench sequence producing Ru(bpy)<sub>3</sub><sup>3+</sup> and MV<sup>++</sup>, phenol oxidation by Ru(bpy)<sub>3</sub><sup>3+</sup> occurs in concert with release of the phenolic O-H proton to imidazole. Thus, the rate determining reaction step leading to the experimentally observable MLCT bleach recoveries (Figure 4, Figure S4) is CPET (orange arrows in Scheme 5, upper line in Scheme 2). CPET has been identified as the prevalent PCET mechanism in many cases of phenol oxidation.<sup>6,11-15,18,19,40,50-64</sup> We note that all thermodynamic considerations made above are based on the phenol oxidation potentials from Figure 1 / Table 1 which were measured in pure CH<sub>3</sub>CN with 0.1 M TBAPF<sub>6</sub>. In the photochemical experiments, however, substantial concentrations of imidazole are present (Figures 4, 5). The presence of base can lower the phenol oxidation potentials significantly, but this is mostly the result of concerted proton-electron release.<sup>52,53</sup> That state of matters provides further support for our mechanistic assignment of CPET rather than ET-PT.

CPET kinetics as a function of phenol– $Ru(bpy)_3^{2+}$  distance. Only phenols which are hydrogen-bonded to imidazole are predisposed for CPET. Consequently, any analysis of the experimentally observable bleach recovery kinetics must take the hydrogen-bonding equilibrium between the phenols and imidazole (eq. 2) into account.

$$PhOH + im \qquad \Rightarrow \qquad PhOH \cdots im \qquad (eq. 2)$$

The observable bleach recovery rate constant  $(k_{obs})$  is a function of the CPET rate constant  $(k_{CPET})$  times the fraction of hydrogen-bonded phenol-imidazole adducts (eq. 3).<sup>5,21</sup>

$$k_{obs} = k_0 + k_Q \cdot [im] + k_{CPET} \cdot [PhOH \cdot \cdot \cdot im] / c_{PhOH}$$
 (eq. 3)

In eq. 3,  $k_0$  is the inherent  ${}^3MLCT$  bleach recovery rate constant for a given dyad in absence of imidazole. The  $k_Q$ ·[im] term describes the undesired side reaction between  $Ru(bpy)_3^{3+}$  and imidazole

(Scheme 2).  $c_{PhOH}$  is the phenol concentration. Under the assumption that the concentration of hydrogen-bonded phenol-imidazole pairs is small compared to the actual concentration of free imidazole, the expression for  $k_{obs}$  can be reformulated to eq. 4 (see Supporting Information for details):<sup>63,65</sup>

$$k_{obs} - k_0 = k_Q \cdot [im] + k_{CPET} \cdot (K_A \cdot [im]) / (1 + K_A \cdot [im])$$
 (eq. 4)

In eq. 4, KA is the association constant for hydrogen-bonded phenol-imidazole adducts as described by eq. 2. The solid lines in Figure 5 are the result of a global two-parameter fit (using K<sub>A</sub> and k<sub>CPET</sub> as adjustable parameters) to the experimental  $k_{obs} - k_0$  vs. [im] data.  $k_Q$  was held at a value of 5.6·10<sup>5</sup> M<sup>-1</sup> s<sup>-1</sup> <sup>1</sup> (Figure S5, see above). The fit occurred globally to all four sets of data (PhOH/D-xy<sub>1</sub>-Ru<sup>2+</sup>, PhOH/Dxy<sub>2</sub>-Ru<sup>2+</sup>) with one common K<sub>A</sub> value. In other words, K<sub>A</sub> was assumed to be independent of bridge length and deuteration. Our attempts to determine KA in an independent manner (e. g., using UV-Vis or IR spectroscopy) were unsuccessful. The abovementioned global fit yields  $K_A = 6.6 \pm 1.3 \text{ M}^{-1}$ , in line with previously determined association constants for phenol-pyridine adducts in benzonitrile. 63,65 The k<sub>CPET</sub> values extracted from the global fit are summarized in Table 3. The most important finding is a decrease of k<sub>CPET</sub> by roughly two orders of magnitude between the shortest dyad and the dyad with two p-xylene spacers. From the data points in Figure 5 it is already evident that for a given dyad and imidazole concentration, k<sub>CPET</sub> is lower for the deuterated phenols than for the ordinary ones. From the global fit with eq. 4 one obtains H/D kinetic isotope effects (KIEs) of 1.5±0.5 for the shortest dyad and  $2.1\pm0.6$  for the dyad with two p-xylene spacers (last column of Table 3). The necessity of assuming a common K<sub>A</sub> value for all four systems considered here is an unavoidable shortfall in this analysis, but in light of the chemical similarity of all four systems relative to each other (variations only in bridge length and O-H vs. O-D functions) it would appear to be a reasonable assumption.

**Table 3.** CPET rate constants extracted from a global fit with eq. 4 to the experimental data in Figure 5.

dyad	k <sub>CPET</sub> , x=H [s <sup>-1</sup> ]	k <sub>CPET,X=D</sub> [s <sup>-1</sup> ]	k <sub>CPET,X=H</sub> /k <sub>CPET,X=D</sub>
PhOX-xy <sub>1</sub> -Ru <sup>2+</sup>	$(2.35\pm0.42)\cdot10^7$	$(1.62\pm0.29)\cdot10^7$	1.5±0.5
PhOX-xy <sub>2</sub> -Ru <sup>2+</sup>	$(5.62\pm0.67)\cdot10^5$	$(2.64\pm0.39)\cdot10^5$	2.1±0.6

In the tunneling regime, electron transfer rates ( $k_{ET}$ ) commonly exhibit an exponential distance dependence which can be described adequately with eq. 5, in particular when the variation of reaction free energy and reorganization energy with increasing distance (d) is small compared to that of the electronic coupling between the donor and the acceptor.<sup>66</sup>

$$k_{ET}(d) = k_{ET}^{(0)} \cdot \exp(-\beta \cdot d)$$
 (eq. 5)

 $k_{ET}^{(0)}$  is the electron transfer rate constant when the donor and the acceptor are in van der Waals contact,  $\beta$  is the distance decay constant. The latter is usually associated with a certain type of a bridge (or intervening medium) separating the donor from the acceptor, but in principle  $\beta$  is dependent on the entire combination of donor, bridge, and acceptor. Assuming eq. 5 can be applied to  $k_{CPET}$  it is possible to extract a  $\beta$ -value for bidirectional CPET in our systems. Ideally  $\beta$  is determined on the basis of a homologous series of variable-length donor-bridge-acceptor molecules, but this is not possible in the present case because CPET is only kinetically competitive with other reactions of  $\beta$  Ru(bpy)3 in the two shortest dyads. Eq. 6 was used to determine the distance decay constant characterizing the decrease of  $\beta$  kcpet between PhOH/D-xy1-Ru<sup>2+</sup> and PhOH/D-xy2-Ru<sup>2+</sup>.

$$\beta = \ln(k_{CPET,xy1}/k_{CPET,xy2})/(d_{xy2} - d_{xy1})$$
 (eq. 6)

In eq. 6,  $k_{CPET,xy1}$  and  $k_{CPET,xy2}$  are the CPET rate constants for the PhOH/D- $xy_1$ -Ru<sup>2+</sup> and PhOH/D- $xy_2$ -Ru<sup>2+</sup> dyads, respectively (Table 3).  $d_{xy1}$  and  $d_{xy2}$  are the (center-to-center) phenol – Ru(bpy)<sub>3</sub><sup>2+</sup> distances in the two systems. The result is a  $\beta$ -value of  $0.87\pm0.09$  Å<sup>-1</sup>.69

Discussion of distance decay constant. The closest possible comparison of the β-value determined for bidirectional CPET in the PhOH-xy<sub>1,2</sub>-Ru<sup>2+</sup>/imidazole system is to phenothiazine-xylene-Ru(bpy)<sub>3</sub><sup>2+</sup> molecules in which a distance decay constant of 0.77 Å<sup>-1</sup> was found for intramolecular electron transfer.  $^{34,68,70}$  Investigations of analogous phenothiazine-xylene-rhenium(I) molecules gave  $\beta = 0.52$  Å<sup>-1</sup>.  $^{34,68,71}$  Electron transfer across un-substituted oligo-*p*-phenylene bridges usually occurs with β-values around 0.4 Å<sup>-1</sup> or even lower.  $^{72,73}$  Our own recent study of bidirectional CPET with PhOH-xy<sub>1,2,3</sub>-Ru<sup>2+</sup> dyads (involving photoexcited Ru(bpy)<sub>3</sub><sup>2+</sup> rather than Ru(bpy)<sub>3</sub><sup>3+</sup> and pyrrolidine instead of imidazole) yielded  $\beta = 0.67\pm0.23$  Å<sup>-1</sup>. Thus, for the same set of molecules, thermal CPET initiating from photogenerated Ru(bpy)<sub>3</sub><sup>3+</sup> is associated with a larger β-value than CPET initiating from photoexcited Ru(bpy)<sub>3</sub><sup>2+</sup>. This discrepancy could be simply a manifestation of different (superexchange-mediated) electronic donor-acceptor couplings.  $^{68,74}$  We have previously observed that electron transfer from a phenothiazine donor across multiple *p*-xylene bridges produces significantly different β-values for thermal and excited-state electron transfer; with photogenerated Ru(bpy)<sub>3</sub><sup>3+</sup> as an electron acceptor we obtained  $\beta = 0.77$  Å<sup>-1</sup> and with a photoexcited [Re(1,10-phenanthroline)(CO)<sub>3</sub>(pyridine)]<sup>+</sup> complex we found  $\beta = 0.52$  Å<sup>-1</sup>. and with a photoexcited [Re(1,10-phenanthroline)(CO)<sub>3</sub>(pyridine)]<sup>+</sup> complex we found  $\beta = 0.52$  Å<sup>-1</sup>.

Clearly the distance decay constant determined herein is one of the largest (possibly the largest) ever reported for an oligo-p-phenylene based donor-bridge-acceptor system. However, the deviation from what has been previously reported for "simple" (i. e., not proton-coupled) electron transfer in phenothiazine-xylene-Ru(bpy)<sub>3</sub><sup>2+</sup> dyads (0.77 Å<sup>-1</sup>) is within the margins of typical variations for a given bridge.

# SUMMARY AND CONCLUSIONS

In the PhOH-xy<sub>n</sub>-Ru<sup>2+</sup> / imidazole / methyl viologen reaction triples with n=1 and n=2 the sequence of photoreactions illustrated by Scheme 2 and the orange arrows in Scheme 5 takes place. The rate determining step leading to phenol oxidation and Ru(bpy)<sub>3</sub><sup>3+</sup> re-reduction is concerted proton-electron transfer. The rate constant for this bidirectional CPET process decreases by roughly two orders of magnitudes between the n = 1 and n = 2 systems, translating to a distance decay constant of  $0.87\pm0.09$  Å<sup>-1</sup>.

There are now two  $\beta$ -values for the electron transfer distance dependence of bidirectional CPET available in the literature. Both of them  $(0.87\pm0.09 \text{ Å}^{-1}, 0.67\pm0.23 \text{ Å}^{-1})^5$  are clearly at the higher end of the usual range for "simple" (i. e., not proton-coupled) electron transfer across oligo-p-phenylene based bridges.<sup>73</sup> From these two distance dependence studies of bidirectional CPET it seems that if an effect of proton motion on the electron transfer distance dependence is present at all, this effect is relatively small.

Assuming the distance dependence of the CPET rates is dominated by the distance dependence of the electronic coupling matrix element ( $H_{AB,CPET}$ ) describing the interaction between the potential energy surfaces of starting materials and CPET products, the relative insensitivity of the  $\beta$ -value to the concerted proton motion is not particularly surprising. This is because  $H_{AB,CPET}$  can be expressed as a product of electronic coupling matrix elements for proton transfer ( $H_{AB,PT}$ ) and for electron transfer ( $H_{AB,ET}$ ). Increasing the electron donor – electron acceptor distance leads to a significant decrease in  $H_{AB,ET}$ , but  $H_{AB,PT}$  is relatively unaffected as the proton donor – proton acceptor distance remains essentially unchanged.

Purely electrostatic effects which in principle could lead to a steeper distance dependence of electron transfer when proton motion occurs concertedly into a different direction appear to be of minor importance. This makes sense because H<sub>AB,ET</sub> is exponentially dependent on the electron donor – electron acceptor distance but the Coloumb attraction between the electron and proton is inversely proportional to their separation distance.

A key message from this paper is that a long electron transfer distance is no obstacle to concerted proton motion into a separate direction. Based on a  $\beta$ -value of  $0.87\pm0.09$  Å<sup>-1</sup> and assuming a reaction rate of  $10^{13}$  s<sup>-1</sup> for reactants in van der Waals contact, bidirectional CPET involving an electron transfer step over 20 Å can in principle occur on the microsecond timescale, an electron transfer step over 25 Å would require milliseconds.

# **EXPERIMENTAL SECTION**

The synthesis and characterization of the PhOH/D-xy<sub>n</sub>-Ru<sup>2+</sup> molecules from Scheme 1 was reported in a recent paper.<sup>5</sup> UV-Vis spectra were measured on a Cary 5000 instrument from Varian, steady-state luminescence spectroscopy was performed on a Fluorolog3 from Horiba Jobin-Yvon with an R928 photomultiplier. For cyclic voltammetry we used a Versastat3-200 potentiostat from Princeton Applied Research. A Pt disk working electrode and two silver wires as quasi-reference and counter-electrodes were employed. Time-resolved luminescence and transient absorption spectroscopy was performed with an LP920-KS instrument from Edinburgh Instruments and the frequency-doubled output of a Quantel Brilliant b Nd:YAG laser.

# **ACKNOWLEDGMENT**

Funding from the Swiss National Science Foundation through grant number 200021\_146231/1 and from the Deutsche Forschungsgemeinschaft through IRTG-1422 is gratefully acknowledged.

### SUPPORTING INFORMATION PARAGRAPH

Additional luminescence and transient absorption data, derivation of the energy-level diagram shown in Scheme 5, derivation of reaction rate expressions in the CPET and PT-ET limits, more detailed discussion of the PT-ET mechanism.

# **REFERENCES**

- (1) Winkler, J. R.; Gray, H. B. Long-Range Electron Tunneling. J. Am. Chem. Soc. 2014, 136, 2930-2939.
- (2) Edwards, P. P.; Gray, H. B.; Lodge, M. T. J.; Williams, R. J. P. Electron Transfer and Electronic Conduction through an Intervening Medium. *Angew. Chem. Int. Ed.* **2008**, *47*, 6758-6765.
- (3) Warren, J. J.; Menzeleev, A. R.; Kretchmer, J. S.; Miller, T. F.; Gray, H. B.; Mayer, J. M. Long-Range Proton-Coupled Electron-Transfer Reactions of Bis(imidazole) Iron Tetraphenylporphyrins Linked to Benzoates. *J. Phys. Chem. Lett.* **2013**, *4*, 519-523.
- (4) Markle, T. F.; Rhile, I. J.; Mayer, J. M. Kinetic Effects of Increased Proton Transfer Distance on Proton-Coupled Oxidations of Phenol-Amines. *J. Am. Chem. Soc.* **2011**, *133*, 17341-17352.
- (5) Chen, J.; Kuss-Petermann, M.; Wenger, O. S. Distance Dependence of Bidirectional Concerted Proton-Electron Transfer in Phenol-Ru(2,2'-bipyridine)<sub>3</sub><sup>2+</sup> Dyads. *Chem. Eur. J.* **2014**, *20*, 4098-4104.
- (6) Kuss-Petermann, M.; Wolf, H.; Stalke, D.; Wenger, O. S. Influence of Donor-Acceptor Distance Variation on Photoinduced Electron and Proton Transfer in Rhenium(I)-Phenol Dyads. *J. Am. Chem. Soc.* **2012**, *134*, 12844-12854.
- (7) Mayer, J. M. Proton-Coupled Electron Transfer: A Reaction Chemist's View. *Annu. Rev. Phys. Chem.* **2004**, *55*, 363-390.

- (8) Weinberg, D. R.; Gagliardi, C. J.; Hull, J. F.; Murphy, C. F.; Kent, C. A.; Westlake, B. C.; Paul, A.; Ess, D. H.; McCafferty, D. G.; Meyer, T. J. Proton-Coupled Electron Transfer. *Chem. Rev.* **2012**, *112*, 4016-4093.
- (9) Costentin, C.; Robert, M.; Savéant, J.-M. Concerted Proton-Electron Transfers: Electrochemical and Related Approaches. *Acc. Chem. Res.* **2010**, *43*, 1019-1029.
- (10) Hammes-Schiffer, S.; Stuchebrukhov, A. A. Theory of Coupled Electron and Proton Transfer Reactions. *Chem. Rev.* **2010**, *110*, 6939-6960.
- (11) Hammarström, L.; Styring, S. Proton-Coupled Electron Transfer of Tyrosines in Photosystem II and Model Systems for Artificial Photosynthesis: The Role of a Redox-Active Link between Catalyst and Photosensitizer. *Energy Environ. Sci.* **2011**, *4*, 2379-2388.
- (12) Irebo, T.; Johansson, O.; Hammarström, L. The Rate Ladder of Proton-Coupled Tyrosine Oxidation in Water: A Systematic Dependence on Hydrogen Bonds and Protonation State. *J. Am. Chem. Soc.* **2008**, *130*, 9194-9195.
- (13) Irebo, T.; Reece, S. Y.; Sjödin, M.; Nocera, D. G.; Hammarström, L. Proton-Coupled Electron Transfer of Tyrosine Oxidation: Buffer Dependence and Parallel Mechanisms. *J. Am. Chem. Soc.* **2007**, *129*, 15462-15464.
- (14) Irebo, T.; Zhang, M.-T.; Markle, T. F.; Scott, A. M.; Hammarström, L. Spanning Four Mechanistic Regions of Intramolecular Proton-Coupled Electron Transfer in a Ru(bpy)<sub>3</sub><sup>2+</sup>-Tyrosine Complex. *J. Am. Chem. Soc.* **2012**, *134*, 16247–16254.
- (15) Magnuson, A.; Berglund, H.; Korall, P.; Hammarström, L.; Åkermark, B.; Styring, S.; Sun, L. C. Mimicking Electron Transfer Reactions in Photosystem II: Synthesis and Photochemical Characterization of a Ruthenium(II) Tris(bipyridyl) Complex with a Covalently Linked Tyrosine. *J. Am. Chem. Soc.* **1997**, *119*, 10720-10725.

- (16) Sjödin, M.; Styring, S.; Åkermark, B.; Sun, L. C.; Hammarström, L. Proton-Coupled Electron Transfer from Tyrosine in a Tyrosine-Ruthenium-tris-bipyridine Complex: Comparison with Tyrosine(z) Oxidation in Photosystem II. *J. Am. Chem. Soc.* **2000**, *122*, 3932-3936.
- (17) Sjödin, M.; Styring, S.; Wolpher, H.; Xu, Y. H.; Sun, L. C.; Hammarström, L. Switching the Redox Mechanism: Models for Proton-Coupled Electron Transfer from Tyrosine and Tryptophan. *J. Am. Chem. Soc.* **2005**, *127*, 3855-3863.
- (18) Sun, L. C.; Burkitt, M.; Tamm, M.; Raymond, M. K.; Abrahamsson, M.; LeGourriérec, D.; Frapart, Y.; Magnuson, A.; Kenéz, P. H.; Brandt, P.; Tran, A.; Hammarström, L.; Styring, S.; Åkermark, B. Hydrogen-Bond Promoted Intramolecular Electron Transfer to Photogenerated Ru(III): A Functional Mimic of Tyrosine(Z) and Histidine 190 in Photosystem II. *J. Am. Chem. Soc.* 1999, *121*, 6834-6842.
- (19) Zhang, M.-T.; Irebo, T.; Johansson, O.; Hammarström, L. Proton-Coupled Electron Transfer from Tyrosine: A Strong Rate Dependence on Intramolecular Proton Transfer Distance. *J. Am. Chem. Soc.* **2011**, *133*, 13224-13227.
- (20) Sjödin, M.; Ghanem, R.; Polivka, T.; Pan, J.; Styring, S.; Sun, L. C.; Sundström, V.; Hammarström, L. Tuning Proton Coupled Electron Transfer from Tyrosine: A Competition between Concerted and Step-wise Mechanisms. *Phys. Chem. Chem. Phys.* **2004**, *6*, 4851-4858.
- (21) Pizano, A. A.; Yang, J. L.; Nocera, D. G. Photochemical Tyrosine Oxidation with a Hydrogen-Bonded Proton Acceptor by Bidirectional Proton-Coupled Electron Transfer. *Chem. Sci.* **2012**, *3*, 2457-2461.
- (22) Reece, S. Y.; Nocera, D. G. Direct Tyrosine Oxidation Using the MLCT Excited States of Rhenium Polypyridyl Complexes. *J. Am. Chem. Soc.* **2005**, *127*, 9448-9458.

- (23) Lachaud, T.; Quaranta, A.; Pellegrin, Y.; Dorlet, P.; Charlot, M. F.; Un, S.; Leibl, W.; Aukauloo, A. A Biomimetic Model of the Electron Transfer between P-680 and the Tyrz-His<sub>190</sub> Pair of PSII. *Angew. Chem. Int. Ed.* **2005**, *44*, 1536-1540.
- (24) Quaranta, A.; Lachaud, F.; Herrero, C.; Guillot, R.; Charlot, M. F.; Leibl, W.; Aukauloo, A. Influence of the Protonic State of an Imidazole-Containing Ligand on the Electrochemical and Photophysical Properties of a Ruthenium(II) Polypyridine-Type Complex. *Chem. Eur. J.* **2007**, *13*, 8201-8211.
- (25) Megiatto, J. D.; Mendez-Hernandez, D. D.; Tejeda-Ferrari, M. E.; Teillout, A. L.; Llansola-Portoles, M. J.; Kodis, G.; Poluektov, O. G.; Rajh, T.; Mujica, V.; Groy, T. L.; Gust, D.; Moore, T. A.; Moore, A. L. A Bioinspired Redox Relay that Mimics Radical Interactions of the Tyr-His Pairs of Photosystem II. *Nat. Chem.* **2014**, *6*, 423-428.
- (26) Hankache, J.; Niemi, M.; Lemmetyinen, H.; Wenger, O. S. Photoinduced Electron Transfer in Linear Triarylamine-Photosensitizer-Anthraquinone Triads with Ruthenium(II), Osmium(II), and Iridium(III). *Inorg. Chem.* **2012**, *51*, 6333-6344.
- (27) Bordwell, F. G.; Cheng, J. P. Substituent Effects on the Stabilities of Phenoxyl Radicals and the Acidities of Phenoxyl Radical Cations. *J. Am. Chem. Soc.* **1991**, *113*, 1736-1743.
- (28) Warren, J. J.; Tronic, T. A.; Mayer, J. M. Thermochemistry of Proton-Coupled Electron Transfer Reagents and its Implications. *Chem. Rev.* **2010**, *110*, 6961-7001.
- (29) Some rapid dimerization of phenoxyl radicals cannot be completely excluded despite the presence of bulky *t*-butyl groups.
- (30) The initial oxidative sweep produces phenoxyl radicals which are reduced to phenolate in the subsequent reductive sweep to potentials below -2.0 V. Re-oxidation of the phenolate to phenoxyl radical is then detected at -0.6 V.

- (31) Braterman, P. S.; Song, J. I. Spectroelectrochemistry of Aromatic Ligands and their Derivatives. 1. Reduction Products of 4,4'-Bipyridine, 2,2'-Bipyridine, 2,2'-Bipyrimidine, and some Quaternized Derivatives. *J. Org. Chem.* **1991**, *56*, 4678-4682.
- (32) Crane, B. R.; Di Bilio, A. J.; Winkler, J. R.; Gray, H. B. Electron Tunneling in Single Crystals of Pseudomonas Aeruginosa Azurins. *J. Am. Chem. Soc.* **2001**, *123*, 11623-11631.
- (33) Walther, M. E.; Wenger, O. S. Tuning the Rates of Long-Range Charge Transfer across Phenylene Wires. *ChemPhysChem* **2009**, *10*, 1203-1206.
- (34) Hanss, D.; Walther, M. E.; Wenger, O. S. Importance of Covalence, Conformational Effects and Tunneling-Barrier Heights for Long-Range Electron Transfer: Insights from Dyads with Oligo-*p*-phenylene, Oligo-*p*-xylene and Oligo-*p*-dimethoxybenzene Bridges. *Coord. Chem. Rev.* **2010**, 254, 2584-2592.
- (35) In Figure 3a the intensity of the MV<sup>++</sup> signal at 395 nm is somewhat higher in the spectrum measured with a 2 μs delay than in the spectrum measured without time delay. This is attributed to fluctuations in laser excitation power.
- (36) Roundhill, D. M. *Photochemistry and Photophysics of Metal Complexes*; Plenum Press: New York, 1994.
- (37) Heath, G. A.; Yellowlees, L. J.; Braterman, P. S. Spectro-Electrochemical Studies on Tris-Bipyridyl Ruthenium Complexes UV, Visible, and Near-Infrared Spectra of the Series Ru(bipyridyl)<sub>3</sub><sup>2+/1+/0/1-</sup>. *J. Chem. Soc., Chem. Commun.* **1981**, 287-289.
- (38) In principle oxidized imidazole and reduced methyl viologen can then react back to the starting materials on a longer time scale, but we did not investigate this.
- (39) Mayer, J. M.; Rhile, I. J.; Larsen, F. B.; Mader, E. A.; Markle, T. F.; DiPasquale, A. G. Models for Proton-Coupled Electron Transfer in Photosystem II. *Photosynth. Res.* **2006**, *87*, 3-20.

- (40) Bonin, J.; Costentin, C.; Robert, M.; Savéant, J. M. Pyridine as Proton Acceptor in the Concerted Proton Electron Transfer Oxidation of Phenol. *Org. Biomol. Chem.* **2011**, *9*, 4064-4069.
- (41) Lind, J.; Shen, X.; Eriksen, T. E.; Merenyi, G. The One-Electron Reduction Potential of 4-Substituted Phenoxyl Radicals in Water. *J. Am. Chem. Soc.* **1990**, *112*, 479-482.
- (42) Das, P. K.; Encinas, M. V.; Steenken, S.; Scaiano, J. C. Reaction of Tert-Butoxy Radicals with Phenols Comparison with the Reactions of Carbonyl Triplets. *J. Am. Chem. Soc.* **1981**, 103, 4162-4166.
- (43) Bjerrum, M. J.; Casimiro, D. R.; Chang, I.-J.; Di Bilio, A. J.; Gray, H. B.; Hill, M. G.; Langen, R.; Mines, G. A.; Skov, L. K.; Winkler, J. R.; Wuttke, D. S. Electron-Transfer in Ruthenium-Modified Proteins. *J. Bioenerg. Biomembr.* **1995**, *27*, 295-302.
- (44) Winkler, J. R.; Gray, H. B. Electron-Transfer in Ruthenium-Modified Proteins. *Chem. Rev.* **1992**, *92*, 369-379.
- (45) He, B.; Wenger, O. S. Ruthenium-Phenothiazine Electron Transfer Dyad with a Photoswitchable Dithienylethene Bridge: Flash-Quench Studies with Methyl Viologen. *Inorg. Chem.* **2012**, *51*, 4335-4342.
- (46) In principle PhO<sup>-</sup>-xy<sub>n</sub>-\*Ru<sup>2+</sup> could also react intramolecularly to form PhO•-xy<sub>n</sub>-Ru<sup>+</sup>. This species is then more likely to react intramolecularly to give PhO<sup>-</sup>-xy<sub>n</sub>-Ru<sup>2+</sup> than to react with methyl viologen to the observed photoproducts.
- (47) Kütt, A.; Leito, I.; Kaljurand, I.; Soovali, L.; Vlasov, V. M.; Yagupolskii, L. M.; Koppel, I. A. A Comprehensive Self-Consistent Spectrophotometric Acidity Scale of Neutral Bronsted Acids in Acetonitrile. *J. Org. Chem.* **2006**, *71*, 2829-2838.
- (48) Bordwell, F. G. Equilibrium Acidities in Dimethyl-Sulfoxide Solution. *Acc. Chem. Res.* **1988**, *21*, 456-463.

- (49) Crampton, M. R.; Robotham, I. A. Acidities of Some Substituted Ammonium Ions in Dimethyl Sulfoxide. *J. Chem. Res.* **1997**, 22-23.
- (50) Sjödin, M.; Irebo, T.; Utas, J. E.; Lind, J.; Merenyi, G.; Åkermark, B.; Hammarström, L. Kinetic Effects of Hydrogen Bonds on Proton-Coupled Electron Transfer from Phenols. *J. Am. Chem. Soc.* **2006**, *128*, 13076-13083.
- (51) Markle, T. F.; Mayer, J. M. Concerted Proton-Electron Transfer in Pyridylphenols: The Importance of the Hydrogen Bond. *Angew. Chem. Int. Ed.* **2008**, *47*, 738-740.
- (52) Rhile, I. J.; Markle, T. F.; Nagao, H.; DiPasquale, A. G.; Lam, O. P.; Lockwood, M. A.; Rotter, K.; Mayer, J. M. Concerted Proton-Electron Transfer in the Oxidation of Hydrogen-Bonded Phenols. *J. Am. Chem. Soc.* **2006**, *128*, 6075-6088.
- (53) Rhile, I. J.; Mayer, J. M. One-Electron Oxidation of a Hydrogen-Bonded Phenol Occurs by Concerted Proton-Coupled Electron Transfer. *J. Am. Chem. Soc.* **2004**, *126*, 12718-12719.
- (54) Schrauben, J. N.; Cattaneo, M.; Day, T. C.; Tenderholt, A. L.; Mayer, J. M. Multiple-Site Concerted Proton-Electron Transfer Reactions of Hydrogen-Bonded Phenols Are Nonadiabatic and Well Described by Semiclassical Marcus Theory. *J. Am. Chem. Soc.* **2012**, *134*, 16635-16645.
- (55) Markle, T. F.; Rhile, I. J.; DiPasquale, A. G.; Mayer, J. M. Probing Concerted Proton-Electron Transfer in Phenol-Imidazoles. *Proc. Natl. Acad. Sci. U. S. A.* **2008**, *105*, 8185-8190.
- (56) Bonin, J.; Costentin, C.; Louault, C.; Robert, M.; Savéant, J. M. Water (in Water) as an Intrinsically Efficient Proton Acceptor in Concerted Proton Electron Transfers. *J. Am. Chem. Soc.* **2011**, *133*, 6668-6674.
- (57) Costentin, C.; Robert, M.; Savéant, J. M. Electrochemical and Homogeneous Proton-Coupled Electron Transfers: Concerted Pathways in the One-Electron Oxidation of a Phenol Coupled with an Intramolecular Amine-Driven Proton Transfer. *J. Am. Chem. Soc.* **2006**, *128*, 4552-4553.

- (58) Costentin, C.; Robert, M.; Savéant, J. M. Concerted Proton-Electron Transfer Reactions in Water. Are the Driving Force and Rate Constant Depending on pH When Water Acts as Proton Donor or Acceptor? *J. Am. Chem. Soc.* **2007**, *129*, 5870-5879.
- (59) Costentin, C.; Robert, M.; Savéant, J. M. Concerted Proton-Electron Transfers in the Oxidation of Phenols. *Phys. Chem. Chem. Phys.* **2010**, *12*, 11179-11190.
- (60) Bonin, J.; Costentin, C.; Louault, C.; Robert, M.; Routier, M.; Savéant, J. M. Intrinsic Reactivity and Driving Force Dependence in Concerted Proton-Electron Transfers to Water Illustrated by Phenol Oxidation. *Proc. Natl. Acad. Sci. U. S. A.* **2010**, *107*, 3367-3372.
- (61) Bronner, C.; Wenger, O. S. Kinetic Isotope Effects in Reductive Excited-State Quenching of Ru(2,2 '-bipyrazine)<sub>3</sub><sup>2+</sup> by Phenols. *J. Phys. Chem. Lett.* **2012**, *3*, 70-74.
- (62) Bronner, C.; Wenger, O. S. Proton-Coupled Electron Transfer between 4-Cyanophenol and Photoexcited Rhenium(I) Complexes with Different Protonatable Sites. *Inorg. Chem.* **2012**, *51*, 8275-8283.
- (63) Biczok, L.; Gupta, N.; Linschitz, H. Coupled Electron-Proton Transfer in Interactions of Triplet C-60 with Hydrogen-Bonded Phenols: Effects of Solvation, Deuteration, and Redox Potentials. *J. Am. Chem. Soc.* **1997**, *119*, 12601-12609.
- (64) Cape, J. L.; Bowman, M. K.; Kramer, D. M. Reaction Intermediates of Quinol Oxidation in a Photoactivatable System that Mimics Electron Transfer in the Cytochrome bc(1) Complex. *J. Am. Chem. Soc.* **2005**, *127*, 4208-4215.
- (65) Biczók, L.; Linschitz, H. Concerted Electron and Proton Movement in Quenching of Triplet C-60 and Tetracene Fluorescence by Hydrogen-Bonded Phenol-Base Pairs. *J. Phys. Chem.* **1995**, 99, 1843-1845.

- (66) Gray, H. B.; Winkler, J. R. Long-Range Electron Transfer. Proc. Natl. Acad. Sci. U. S. A. 2005, 102, 3534-3539.
- (67) Albinsson, B.; Eng, M. P.; Pettersson, K.; Winters, M. U. Electron and Energy Transfer in Donor-Acceptor Systems with Conjugated Molecular Bridges. *Phys. Chem. Chem. Phys.* **2007**, *9*, 5847-5864.
- (68) Wenger, O. S. How Donor-Bridge-Acceptor Energetics Influence Electron Tunneling Dynamics and Their Distance Dependences. *Acc. Chem. Res.* **2011**, *44*, 25-35.
  - (69) The error here reflects the uncertainty in the  $k_{CPET}$  values from Table 3.
- (70) Hanss, D.; Wenger, O. S. Tunneling Barrier Effects on Photoinduced Charge Transfer through Covalent Rigid Rod-Like Bridges. *Inorg. Chem.* **2009**, *48*, 671-680.
- (71) Hanss, D.; Wenger, O. S. Electron Tunneling through Oligo-p-xylene Bridges. *Inorg. Chem.* **2008**, *47*, 9081-9084.
- (72) Weiss, E. A.; Ahrens, M. J.; Sinks, L. E.; Gusev, A. V.; Ratner, M. A.; Wasielewski, M. R. Making a Molecular Wire: Charge and Spin Transport through Para-phenylene Oligomers. *J. Am. Chem. Soc.* **2004**, *126*, 5577-5584.
- (73) Wenger, O. S. Photoinduced Electron and Energy Transfer in Phenylene Oligomers. *Chem. Soc. Rev.* **2011**, *40*, 3538-3550.
- (74) Eng, M. P.; Albinsson, B. Non-Exponential Distance Dependence of Bridge-Mediated Electronic Coupling. *Angew. Chem. Int. Ed.* **2006**, *45*, 5626-5629.

# SYNOPSIS TOC

The dependence of reaction rates for bidirectional concerted proton-electron transfer on the electron donor – electron acceptor distance is similar to that for "simple" (= not proton-coupled) electron transfer.

